Physical Science International Journal
6(3): 144-162, 2015, Article no.PSIJ.2015.041
ISSN: 2348-0130

SCIENCEDOMAIN *international*
www.sciencedomain.org

MHD Flow of Fluid over a Rotating Inclined Permeable Plate with Variable Reactive Index

Mohammad Wahiduzzaman[1*], Md. Shakhaoath Khan[2], Ifsana Karim[2], Pallab Biswas[1] and Md. Sharif Uddin[1]

[1]Mathematics Discipline, Science Engineering and Technology School, Khulna University, Khulna 9208, Bangladesh.
[2]Discipline of Chemical Engineering, The University of Newcastle, Callaghan, NSW 2308, Australia.

Authors' contributions

This work was carried out in collaboration between all authors. Authors designed the study, wrote the protocol, and wrote the first draft of the manuscript. The funding, overall suggestions, proof reading was also done by all authors and approved the final manuscript.

Article Information

DOI: 10.9734/PSIJ/2015/15194
Editor(s):
(1) Yang-Hui He, Dept. of Mathematics, University of Oxford, UK and Reader in Mathematics, City University, London, UK,
(2) Stefano Moretti, School of Physics & Astronomy, University of Southampton, UK.
Reviewers:
(1) Anselm O. Oyem, Department of Mathematics, Federal University Lokoja, Lokoja, Nigeria.
(2) Anonymous, China.
(3) Anonymous, Algeria.
(3) Anonymous, Malaysia.
Complete Peer review History: http://www.sciencedomain.org/review-history.php?iid=1000&id=33&aid=8271

Original Research Article

Received 12th November 2014
Accepted 2nd February 2015
Published 26th February 2015

ABSTRACT

MHD free convection, heat and mass transfer flow over a rotating inclined permeable plate with the influence of magnetic field, thermal radiation and chemical reaction of various order has been investigated numerically. The governing boundary-layer equations are formulated and transformed into a set of similarity equations with the help of similarity variables derived by lie group transformation. The governing equations are solved numerically using the Nactsheim-Swigert Shooting iteration technique together with the Runge-Kutta six order iteration schemes. The simulation results are presented graphically to illustrate influence of magnetic parameter (M), porosity parameter (γ), rotational parameter (R'), Grashof number (G_r), modified Grashof number (G_m), thermal conductivity parameter (T_c), Prandtl number (P_r), radiation parameter (R), heat source parameter (Q), Eckert number (E_c), Schmidt number (S_c), reaction parameter (λ)

**Corresponding author: Email: wahidmathku@gmail.com;*

andorder of chemical reaction (n) on the all fluid velocity components, temperature and concentration distribution as well as Skin-friction coefficient, Nusselt and Sherwood number at the plate.

Keywords: MHD; inclined permeable plate; thermal radiation; chemical reaction.

NOMENCLATURE

B_0 *Constant magnetic flux density*
C *Constant depends on the properties of the fluid*
C *Concentration of the fluid*
C_p *Specific heat at constant pressure*
D_m *Mass diffusivity*
f' *Dimensionless primary velocity*
g *Acceleration due to gravity*
g_0 *Dimensionless secondary velocity*
K *Thermal conductivity*
k_∞ *Undisturbed thermal conductivity*
k_0 *Reaction rate*
K *Permeability of the porous medium*
N *Order of chemical reaction*
P *Pressure distribution in the boundary layer*
q_r *Radiative heat flux in the y direction*
Q_T *Heat generation*
Q_0 *Heat source*
T *Time*
T *Fluid temperature*
U *Uniform velocity*
u, v *Velocity components along x and y axes respectively*
x' *Dimensionless axial distance along x axis*

DIMENSIONLESS PARAMETERS

E_c *Eckert number*
R' *Rotational parameter*
G_r *Grashof number*
G_m *Modified Grashof number*
M *Magnetic parameter*
P_r *Prandtl number*
Q *Heat source parameter*
R *Radiation parameter*
S_c *Schmidt number*
T_c *Thermal conductivity parameter*
γ *Permeability of the porous medium*
λ *Reaction parameter*

GREEK SYMBOLS

υ *Kinematic viscosity of the fluid*
μ *Dynamic viscosity of the fluid*

σ *Electrical conductivity*
σ_0 *Constant electrical conductivity*
σ_s *Stefan-Boltzmann constant*
ρ *Density of the fluid*
α *Thermal diffusivity*
$\alpha_1 - \alpha_6$ *Arbitrary real number*
β *Inclination angle*
β_T *Thermal expansion coefficient*
β_C *Concentration expansion coefficient*
κ^* *Mean absorption coefficient*
ε *Parameter of the group*
ψ *Stream function*
η *Similarity variable*
θ *Dimensionless temperature*
φ *Dimensionless concentration*
Ω *Angular velocity of the plate*

SUBSCRIPTS

w *Condition of the wall*
∞ *Condition of the free steam*

1. INTRODUCTION

Coupled heat and mass transfer problems in the presence of chemical reactions are of importance in many processes and have, therefore, received considerable amount of attention of researchers in recent years. Chemical reactions can occur in processes such as drying, distribution of temperature and moisture over agricultural fields and groves of fruit trees, damage of crops due to freezing, evaporation at the surface of a water body, energy transfer in a wet cooling tower and flow in a desert cooler. Chemical reactions are classified as either homogeneous or heterogeneous processes. A homogeneous reaction is one that occurs uniformly throughout a given phase. On the other hand, a heterogeneous reaction takes a restricted area or within the boundary of a phase. Analysis of the transport processes and their interaction with chemical reactions is quite difficult and closely related to fluid dynamics. Chemical reaction effects on heat and mass transfer has been analyzed by many researchers over various geometries with various boundary conditions in porous and nonporous media. Symmetry groups or simply symmetries are invariant transformations that do not alter the structural form of the equation under investigation which is described by Bluman and Kumei [1]. MHD boundary layer equations for power law fluids with variable electric conductivity is studied by Helmy [2]. In the case of a scaling group of transformations, the group-invariant solutions are nothing but the well known similarity solutions which is studied by Pakdemirli and Yurusoy [3]. Symmetry groups and similarity solutions for free convective boundary-layer problem was studied by Kalpakides and Balassas [4]. Makinde [5] investigated the effect of free convection flow with thermal radiation and mass transfer past moving vertical porous plate. Seddeek and Salem [6] investigated the Laminar mixed convection adjacent to vertical continuously stretching sheet with variable viscosity and variable thermal diffusivity. Ibrahim, Elaiw and Bakr [7] studied the effect of the chemical reaction and radiation absorption on the unsteady MHD free convection flow past a semi infinite vertical permeable moving plate with heat source and suction. El-Kabeir, El-Hakiem and Rashad [8] studied Lie group analysis of unsteady MHD three dimensional dimensional by natural convection from an inclined stretching surface saturated porous medium. Rajeswari, Jothiram and Nelson [9] studied the effect of chemical reaction, heat and mass transfer on nonlinear MHD boundary layer flow through a vertical porous surface in the presence of suction. Chandrakala [10] investigated chemical reaction effects on MHD flow past an impussively started semi-infinite vertical plate. Joneidi, Domairry and Babaelahi [11] studied analytical treatment of MHD free convective flow and mass

transfer over a stretching sheet with chemical reaction. Muhaimin, Kandasamy and Hashim [12] studied the effect of chemical reaction, heat and mass transfer on nonlinear boundary layer past a porous shrinking sheet in the presence of suction. Rahman and Salahuddin [13] studied hydromagnetic heat and mass transfer flow over an inclined heated surface with variable viscosity and electric conductivity. Very recently a number of studies of MHD heat and mass transfer boundary layer fluid flow with the various effects of physical parameter reported in the literature [14-27]. As per standard text and works of previous researchers, the radiative flow of an electrically conducting fluid and heat and mass transfer situation arises in many practical applications such as in electrical power generation, astrophysical flows, solar power technology, space vehicle re-entry, nuclear reactors.

The objective of this study is to present a similarity analysis of boundary layer flow past a rotating inclined permeable plate with the influence of magnetic field, thermal radiation, thermal conductivity and chemical reaction of various orders.

2. MATHEMATICAL MODEL OF THE FLOW AND GOVERNING EQUATIONS

Steady two dimensional MHD heat and mass transfer flow with chemical reaction and radiation over an inclined permeable plate $y=0$ in a rotating system under the influence of transversely applied magnetic field is considered. The sketch of the physical configuration and coordinate system are shown in Fig. 1. The *x*-axis is taken in the upward direction and *y*-axis is normal to it. Again the plate is inclined at an angle β with the *x*-axis. The flow takes place at $y \geq 0$, where *y* is the coordinate measured normal to the *x*-axis. Initially we consider the plate as well as the fluid is at rest with the same velocity $U\left(=U_\infty\right)$, temperature $T\left(=T_\infty\right)$ and concentration $C\left(=C_\infty\right)$. Also it is assumed that the fluid and plate is at rest after that the whole system is allowed to rotate with a constant angular velocity $R=(0,-\Omega,0)$ about the y-axis and then the temperature and species concentration of the plate are raised to $T_w\left(>T_\infty\right)$ and $C_w\left(>C_\infty\right)$ respectively, which are thereafter maintained constant, where T_w and C_w is the temperature and concentration respectively at wall and T_∞ and C_∞ is the temperature and concentration respectively far away from the plate.

The electrical conductivity is assumed to vary with the velocity of the fluid and have the form [2],

$\sigma=\sigma_0 u$, σ_0 is the constant electrical conductivity.

The applied magnetic field strength is considered, as follows [13]

$$B(x)=\frac{B_0}{\sqrt{x}}$$

The temperature dependent thermal conductivity is assumed to vary linearly, as follows [6]

$$k(T)=k_\infty\left[1+c\left(T-T_\infty\right)\right]$$

Where k_∞ is the undisturbed thermal conductivity and c is the constant depending on the properties of the fluid.

The governing equations for the continuity, momentum, energy and concentration in laminar MHD incompressible boundary-layer flow is presented follows

$$\frac{\partial u}{\partial x}+\frac{\partial v}{\partial y}=0 \tag{1}$$

$$u\frac{\partial u}{\partial x}+v\frac{\partial u}{\partial y}=\upsilon\frac{\partial^2 u}{\partial y^2}+2\Omega w-\frac{\upsilon}{K}u-\frac{\sigma_0 B_0^2 u^2}{\rho x}+g\beta_T\left(T-T_\infty\right)\cos\beta+g\beta_C\left(C-C_\infty\right)\cos\beta \tag{2}$$

$$u\frac{\partial w}{\partial x}+v\frac{\partial w}{\partial y}=\upsilon\frac{\partial^2 w}{\partial y^2}-2\Omega u-\frac{\upsilon}{K}w-\frac{\sigma_0 B_0^2 u w}{\rho x} \tag{3}$$

$$u\frac{\partial T}{\partial x}+v\frac{\partial T}{\partial y}=\frac{1}{\rho C_p}\frac{\partial}{\partial y}\left[k(T)\frac{\partial T}{\partial y}\right]+\frac{Q_0(T-T_\infty)}{\rho C_p}-\frac{\alpha}{k_\infty}\left(\frac{\partial q_r}{\partial y}\right)+\frac{\upsilon}{C_p}\left(\frac{\partial u}{\partial y}\right)^2 \tag{4}$$

$$u\frac{\partial C}{\partial x}+v\frac{\partial C}{\partial y}=D_m\frac{\partial^2 C}{\partial y^2}-k_0(C-C_\infty)^n \tag{5}$$

and the boundary conditions for the model is

$$\left.\begin{array}{l} u=U, v=0, w=0, T=T_w, C=C_w \quad \text{at } y=0 \\ u\to 0, w\to 0, T\to T_\infty, C\to C_\infty \quad \text{as } y\to\infty \end{array}\right\} \tag{6}$$

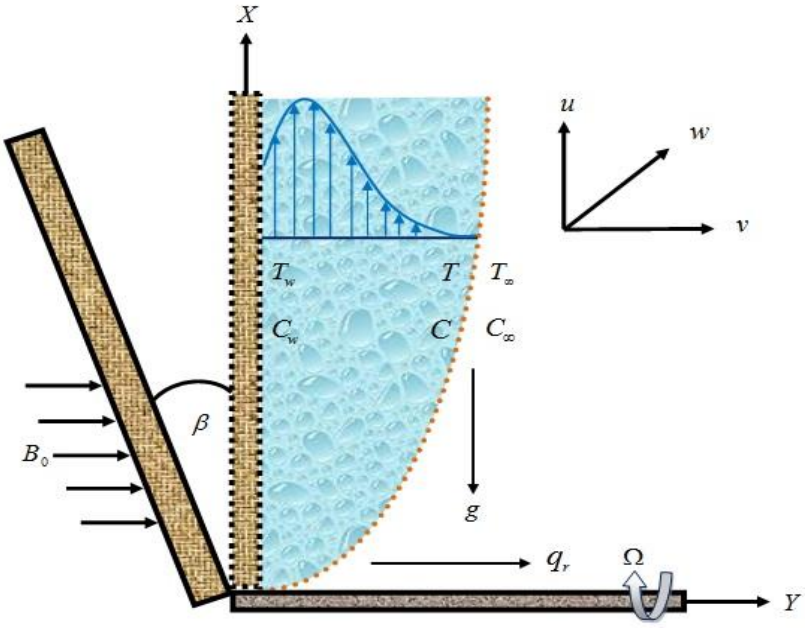

Fig. 1. Physical configuration of the flow

where, *U* is the uniform velocity, β is the inclination angle of the plate with *x*-axis, C_p is the specific heat at constant pressure, $k(T)$ is the temperature dependent thermal conductivity, Q_0 is the heat source, D_m is the mass diffusivity, k_0 is the reaction rate, $k_0>0$ for destructive reaction, $k_0=0$ for no reaction and $k_0<0$ for generative reaction, *n* (integer) is the order of chemical reaction, q_r is the chemical reaction parameter, T_w and C_w is the temperature and concentration respectively at wall and T_∞ and C_∞ is the temperature and concentration respectively far away from the plate.

2.1 Method of Solution

Introducing the following dimensionless variables

$$x'=\frac{xU}{\upsilon}, y'=\frac{yU}{\upsilon}, u'=\frac{u}{U}, v'=\frac{v}{U}, w'=\frac{w}{U}, \theta=\frac{T-T_\infty}{T_w-T_\infty}$$

and $\varphi=\dfrac{C-C_\infty}{C_w-C_\infty}$

the following equations are obtained,

$u=Uu', v=Uv', w=Uw', T=T_\infty+(T_w-T_\infty)\theta$ and

$$C=C_\infty+(C_w-C_\infty)\varphi \tag{7}$$

Now, by using equation (7), the equations (1), (2), (3), (4) and (5) are transformed to

$$\frac{\partial u'}{\partial x'}+\frac{\partial v'}{\partial y'}=0 \tag{8}$$

$$u'\frac{\partial u'}{\partial x'}+v'\frac{\partial u'}{\partial y'}=\frac{\partial^2 u'}{\partial y'^2}+2R'w'-\gamma u'-\frac{M\,u'^2}{x'}+G_r\,\theta cos\beta+G_m\,\varphi cos\beta \tag{9}$$

$$u'\frac{\partial w'}{\partial x'}+v'\frac{\partial w'}{\partial y'}=\frac{\partial^2 w'}{\partial y'^2}-2R'u'-\gamma w'-\frac{M\,u'w'}{x'} \tag{10}$$

$$u'\frac{\partial \theta}{\partial x'}+v'\frac{\partial \theta}{\partial y'}-\frac{1}{P_r}\left[\left(1+T_c\,\theta+R\right)\frac{\partial^2\theta}{\partial y'^2}+T_c\left(\frac{\partial\theta}{\partial y'}\right)^2\right]-Q\theta-E_c\left(\frac{\partial u}{\partial y}\right)^2=0 \tag{11}$$

$$u'\frac{\partial \varphi}{\partial x'}+v'\frac{\partial \varphi}{\partial y'}-\frac{1}{S_c}\frac{\partial^2\varphi}{\partial y'^2}+\lambda\varphi^n=0 \tag{12}$$

using equation (7), the boundary condition (6) becomes,

$$\left.\begin{array}{l} u'=1,v'=0,w'=0,\theta=1,\varphi=1 \ \text{ at } y'=0 \\ u'\to 0,w'\to 0,\theta\to 0,\varphi\to 0 \ \text{ as } y'\to\infty \end{array}\right\} \tag{13}$$

Where,

$$R'=\frac{\Omega\upsilon}{U^2},\gamma=\frac{\upsilon^2}{KU^2},M=\frac{\sigma_0 B_0^2}{\rho},G_r=\frac{g\beta_T\left(T_w-T_\infty\right)\upsilon}{U^3},G_m=\frac{g\beta_c\left(C_w-C_\infty\right)\upsilon}{U^3},T_c=c\left(T_w-T_\infty\right),$$

$$R=\frac{16\sigma_S T_\infty^3}{3\kappa^* k_\infty},P_r=\frac{\upsilon}{\alpha},Q=\frac{Q_0\upsilon}{\rho C_p U^2},E_c=\frac{U^2}{C_p\left(T_w-T_\infty\right)},S_c=\frac{\upsilon}{D_m}\text{ and }\lambda=\frac{k_0\left(C_w-C_\infty\right)^{n-1}\upsilon}{U^2}$$

In order to deal with the problem, we introduce the stream function ψ (since the flow is incompressible) defined by

$$u'=\frac{\partial\psi}{\partial y'},v'=-\frac{\partial\psi}{\partial x'} \tag{14}$$

The mathematical significance of using equation (14) is that the continuity equation (8) is satisfied automatically.

by equation (14), equations (9), (10), (11) and (12) transformed as follows,

$$\frac{\partial\psi}{\partial y'}\frac{\partial^2\psi}{\partial x'\partial y'}-\frac{\partial\psi}{\partial x'}\frac{\partial^2\psi}{\partial y'^2}-\frac{\partial^3\psi}{\partial y'^3}-2R'w'+\gamma\frac{\partial\psi}{\partial y'}+\frac{M}{x'}\left(\frac{\partial\psi}{\partial y'}\right)^2-G_r\theta cos\beta-G_m\varphi cos\beta=0 \tag{15}$$

$$\frac{\partial\psi}{\partial y'}\frac{\partial w'}{\partial x'}-\frac{\partial\psi}{\partial x'}\frac{\partial w'}{\partial y'}-\frac{\partial^2 w'}{\partial y'^2}+2R'\frac{\partial\psi}{\partial y'}+\gamma w'+\frac{M}{x'}\frac{\partial\psi}{\partial y'}w'=0 \tag{16}$$

$$\frac{\partial \psi}{\partial y'}\frac{\partial \theta}{\partial x'}-\frac{\partial \psi}{\partial x'}\frac{\partial \theta}{\partial y'}-\frac{1}{P_r}\left[(1+T_c\,\theta+R)\frac{\partial^2\theta}{\partial y'^2}+T_c\left(\frac{\partial \theta}{\partial y'}\right)^2\right]-Q\,\theta-E_c\left(\frac{\partial^2\psi}{\partial y'^2}\right)^2=0 \tag{17}$$

$$\frac{\partial \psi}{\partial y'}\frac{\partial \varphi}{\partial x'}-\frac{\partial \psi}{\partial x'}\frac{\partial \varphi}{\partial y'}-\frac{1}{S_c}\frac{\partial^2\varphi}{\partial y'^2}+\lambda\,\varphi^n=0 \tag{18}$$

and the boundary conditions (13) become,

$$\left.\begin{aligned}&\frac{\partial \psi}{\partial y'}=1,\frac{\partial \psi}{\partial x'}=0,w'=0,\theta=1,\varphi=1 \text{ at } y'=0\\&\frac{\partial \psi}{\partial y'}\to 0,w'\to 0,\theta\to 0,\varphi\to 0 \quad \text{as } y'\to\infty\end{aligned}\right\} \tag{19}$$

Finding the similarity solution of the equations (15) to (18) is equivalent to determining the invariant solutions of these equations under a particular continuous one parameter group. Introducing the simplified form of Lie-group transformations [8] namely, the scaling group of transformations

$$G_1:\ x^*=x'e^{\varepsilon\alpha_1},y^*=y'e^{\varepsilon\alpha_2},\psi^*=\psi e^{\varepsilon\alpha_3},w^*=w'e^{\varepsilon\alpha_4},\theta^*=\theta\,e^{\varepsilon\alpha_5} \text{ and } \varphi^*=\varphi\,e^{\varepsilon\alpha_6} \tag{20}$$

Here, $\varepsilon(\neq 0)$ is the parameter of the group and $\alpha's$ are arbitrary real numbers whose interrelationship will be determined by our analysis. Equations (20) may be considered as a point transformation which transforms the coordinates $(x',y',\psi,w',\theta,\varphi)$ to the coordinates $(x^*,y^*,\psi^*,w^*,\theta^*,\varphi^*)$.

The system will remain invariant under the group transformation G_1, so the following relations among the exponents are obtained from equations (15) to (18),

$$\left.\begin{aligned}&\alpha_1+2\alpha_2-2\alpha_3=3\alpha_2-\alpha_3=-\alpha_4=\alpha_2-\alpha_3=-\alpha_5=-\alpha_6\\&\alpha_1+\alpha_2-\alpha_3-\alpha_4=2\alpha_2-\alpha_4=\alpha_2-\alpha_3=-\alpha_4\\&\alpha_1+\alpha_2-\alpha_3-\alpha_5=2\alpha_2-\alpha_5=2\alpha_2-2\alpha_5=4\alpha_2-2\alpha_3\\&\alpha_1+\alpha_2-\alpha_3-\alpha_6=2\alpha_2-\alpha_6=-n\alpha_6\end{aligned}\right\} \tag{21}$$

Again, the following relations are obtained from the boundary conditions (19),

$$\left.\begin{aligned}&\alpha_2=\alpha_3\\&\alpha_5=\alpha_6=0\end{aligned}\right\} \tag{22}$$

Solving the system of linear equations (21) and (22), the following relationship are obtained,

$$\alpha_1=2\alpha_2=2\alpha_3,\ \alpha_4=\alpha_5=\alpha_6=0$$

by using the above relation the equation (20) reduces to the following group of transformation

$$x^*=x'e^{2\varepsilon\alpha_2},y^*=y'e^{\varepsilon\alpha_2},\psi^*=\psi e^{\varepsilon\alpha_2},w^*=w',\theta^*=\theta,\varphi^*=\varphi \tag{23}$$

expanding equation (23) by Taylor's method in powers of ε and keeping terms up to the order ε, we have

$$x^*-x'=2\varepsilon x'\alpha_2,y^*-y'=\varepsilon y'\alpha_2,\psi^*-\psi=\varepsilon\psi\alpha_2,w^*-w'=0,\theta^*-\theta=0,\varphi^*-\varphi=0$$

In terms of differentials

$$\frac{dx'}{2\alpha_2 x'}=\frac{dy'}{\alpha_2 y'}=\frac{d\psi}{\alpha_2\psi}=\frac{dw'}{0}=\frac{d\theta}{0}=\frac{d\varphi}{0} \tag{24}$$

Solving the equation (24) the following similarity variables are introduced,

$\eta=\dfrac{y'}{\sqrt{x'}}$, $\psi=\sqrt{x'}f(\eta),w'=g_0(\eta),\theta=\theta(\eta)$ and $\varphi=\varphi(\eta)$

By using the above mentioned variables, equations (15), (16), (17) and (18) becomes

$$f'''+\frac{1}{2}ff''-Mf'^2+2R'g_0-\gamma f'+G_r\,\theta\cos\beta+G_m\,\varphi\cos\beta=0 \tag{25}$$

$$g_0''+\frac{1}{2}fg_0'-2R'f'-\gamma g_0-Mf'g_0=0 \tag{26}$$

$$\frac{1}{P_r}(1+T_c\theta+R)\theta''+\frac{1}{P_r}T_c\theta'^2+\frac{1}{2}f\theta'+Q\theta+E_cf''^2=0 \quad (27)$$

$$\frac{1}{S_c}\varphi''+\frac{1}{2}f\varphi'-\lambda\varphi^n=0 \quad (28)$$

The corresponding boundary conditions (19) become

$$\left.\begin{array}{l} f'=1, f=0, g_0=0, \theta=1, \varphi=1 \text{ at } \eta=0 \\ f'\to 0, g_0\to 0, \theta\to 0, \varphi\to 0 \text{ as } \eta\to\infty \end{array}\right\} \quad (29)$$

where primes denote differentiation with respect to η only and the parameters are defined as

$M=\frac{\sigma_0 B_0^2}{\rho}$ is the magnetic parameter,

$\gamma=\frac{\upsilon^2 x'}{KU^2}$ is the porosity parameter

$R'=\frac{\Omega\upsilon x'}{U^2}$ is the rotational parameter

$G_r=\frac{g\beta_T(T_w-T_\infty)\upsilon x'}{U^3}$ is the Grashof number

$G_m=\frac{g\beta_c(C_w-C_\infty)\upsilon x'}{U^3}$ is the modified Grashof number

$T_c=c(T_w-T_\infty)$ is the thermal conductivity parameter

$P_r=\frac{\upsilon}{\alpha}$ is the Prandtl number

$R=\frac{16\sigma_s T_\infty^3}{3\kappa^* k_\infty}$ is the radiation parameter

$Q=\frac{Q_0\upsilon}{\rho C_p U^2}$ is the heat source parameter

$E_c=\frac{U^2}{C_p(T_w-T_\infty)}$ is Eckert number

$S_c=\frac{\upsilon}{D_m}$ is the Schmidt number

$\lambda=\frac{k_0(C_w-C_\infty)^{n-1}\upsilon}{U^2}$ is the reaction parameter

and n (integer) is the order of chemical reaction

2.2 Skin-friction Coefficients, Nusselt and Sherwood Number

The physical quantities of the skin-friction coefficients, the reduced Nusselt number and reduced Sherwood number are calculated respectively by the following equations,

$$C_f(R_e)^{\frac{1}{2}}=-f''(0) \quad (30)$$

$$C_{g_0}(R_e)^{\frac{1}{2}}=-g_0'(0) \quad (31)$$

$$N_u(R_e)^{-\frac{1}{2}}=-\theta'(0) \quad (32)$$

$$S_h(R_e)^{-\frac{1}{2}}=-\varphi'(0) \quad (33)$$

Where, $R_e=\frac{Ux'}{\upsilon}$ is the Reynolds number.

3. RESULTS AND DISCUSSION

Heat and mass transfer problem associated with laminar flow past an inclined plate of a rotating system are studied in this work. In order to investigated the physical representation of the problem, the numerical values of primary velocity, secondary velocity, temperature and species concentration from equations (25), (26), (27) and (28) with the boundary layer have been computed for different parameters as the magnetic parameter (M), the rotational parameter (R'), the porosity parameter (γ), the Grashof number (G_r), the modified Grashof number (G_m), the radiation parameter (R), the Prandtl number (P_r), the Eckert number (E_c), the thermal conductivity parameter (T_c), the heat source parameter (Q), the Schmidt number (S_c), the reaction parameter (λ), the inclination angle (β) and the order of chemical reaction (n) respectively.

Figs. 2a and 2b show that with the increases of magnetic parameter, primary velocity profiles decreases but secondary velocity profiles increases. Figs. 3a-3d represents that with the

increase of rotational parameter, primary velocity decreases but secondary velocity, temperature and concentration profiles increases.

In Figs. 4a-4d, primary velocity profiles decreases but the secondary velocity, temperature and concentration profiles increases with the increase of porosity parameter. With the increase of inclination angle, primary velocity profiles decreases but secondary velocity profiles increases (Figs. 5a and 5b).

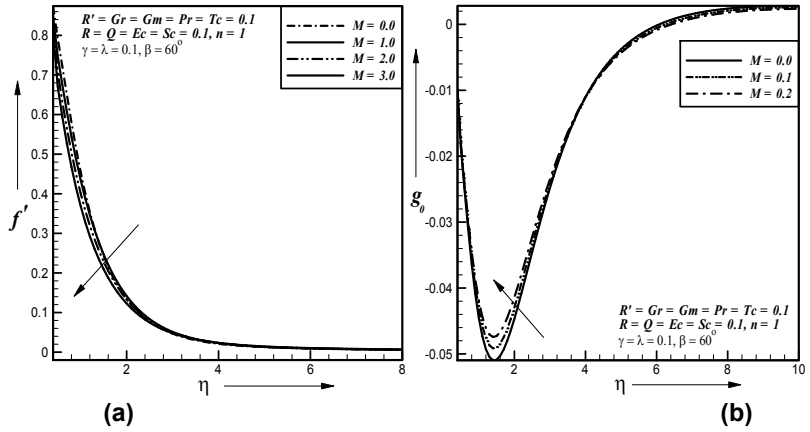

Fig. 2. Effect of magnetic parameter on a) primary velocity b) secondary velocity profiles

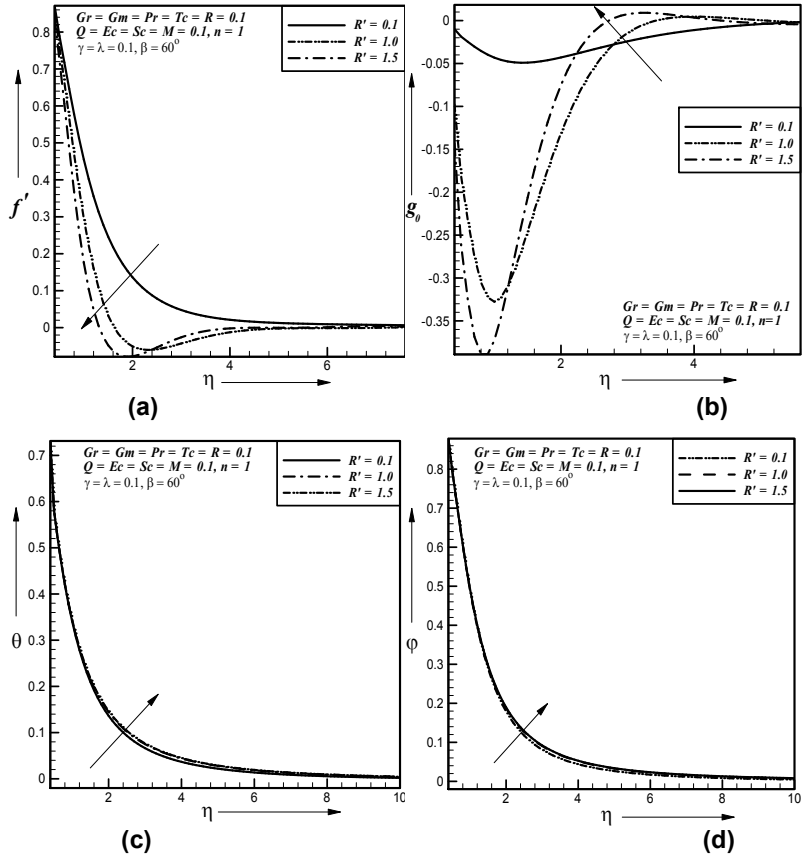

Fig. 3. Effect of rotational parameter on a) primary velocity b) secondary velocity c) temperature d) concentration profiles

In Figs. 6a-6c, we see that with the increase of Grashof number, primary velocity profiles increases but secondary velocity and temperature profiles decreases. Figs. 7a-7c show that with the increase of modified Grashof number, primary velocity profiles increases but secondary velocity and concentration profiles decreases. With the increase of Prandtl number, primary velocity profiles increases but temperature decreases (Figs. 8a and 8b).

Fig. 9a, It is observe that the primary velocity profile increases with the increase of Eckert number. In Fig. 9b, temperature profile increases with the increase of Thermal conductivity parameter.

In Fig. 10a, concentration profiles decreases with the increase of Schmidt number. Fig. 10b represents no reaction $(\lambda = 0.0)$ and destructive reaction $(\lambda > 0.0)$, where the concentration profiles decreases with the increase of reaction parameter.

For the physical interest of the problem, the dimensionless skin-friction coefficient $(-f'')(-g_0')$, the dimensionless heat transfer rate $(-\theta')$ and the dimensionless mass transfer rate $(-\varphi')$ at the plate are plotted against Heat source parameter (Q) and illustrated in Figs. 11-19.

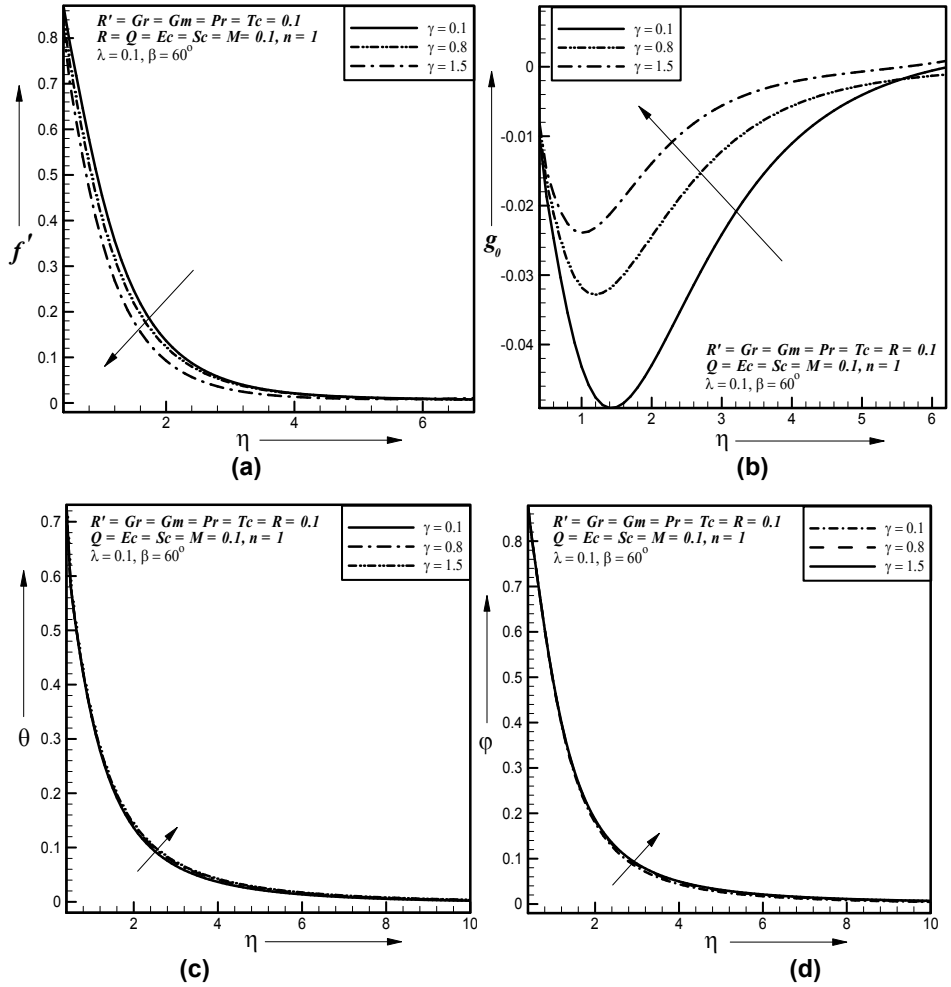

Fig. 4. Effect of porosity parameter on a) primary velocity b) secondary velocity c) temperature d) concentration profiles

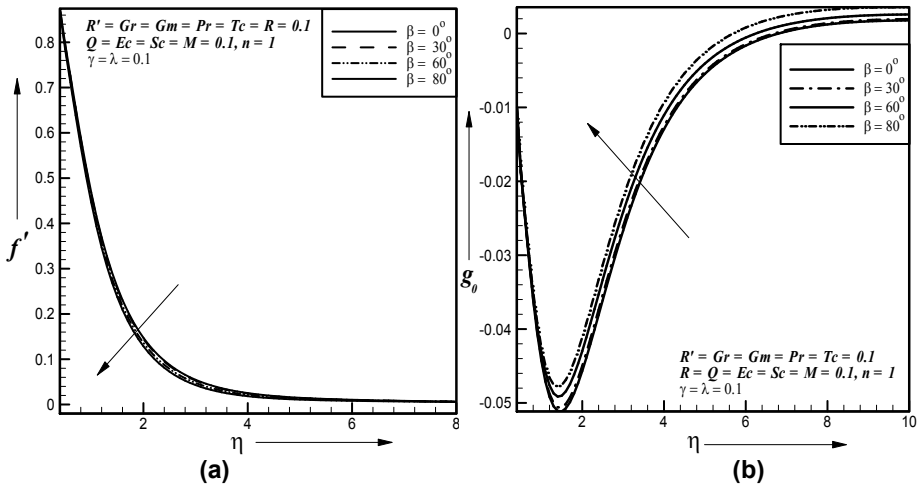

Fig. 5. Effect of inclination angle on a) primary velocity b) secondary velocity profiles

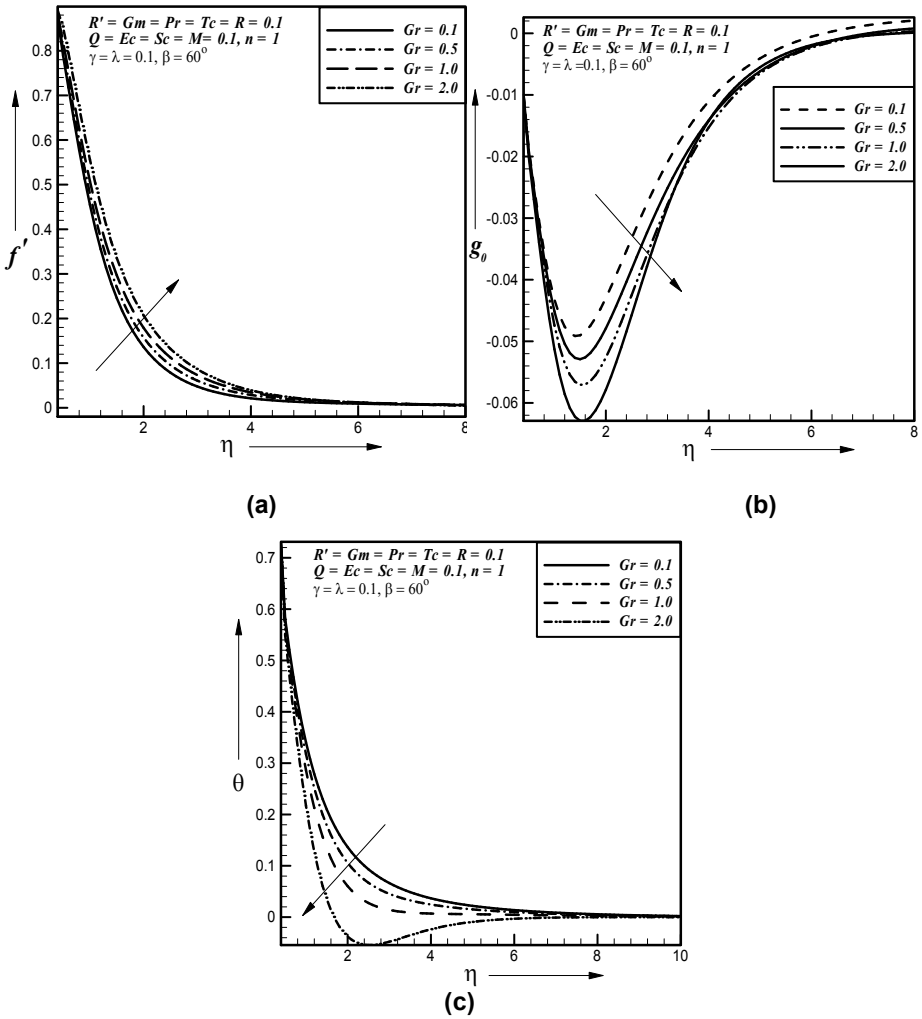

Fig. 6. Effect of Grashof number on a) primary velocity b) secondary velocity c) temperature profiles

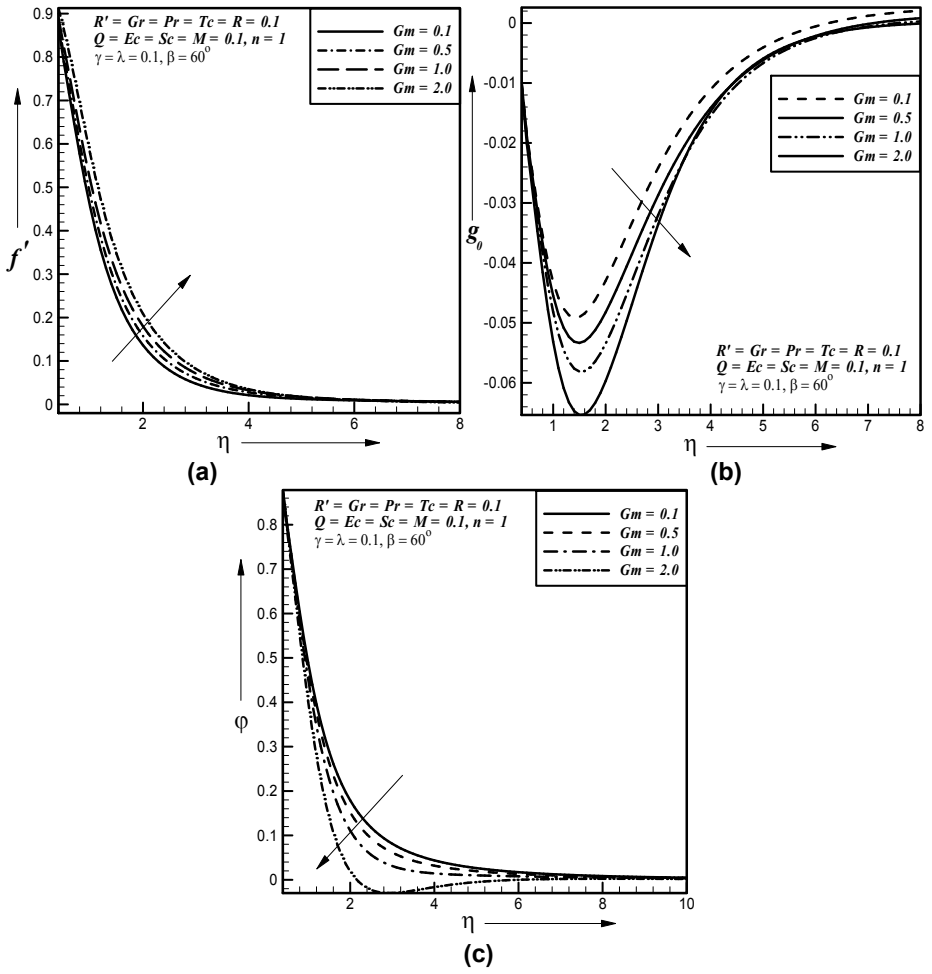

Fig. 7. Effect of modified Grashof number on a) primary velocity b) secondary velocity c) concentration profiles

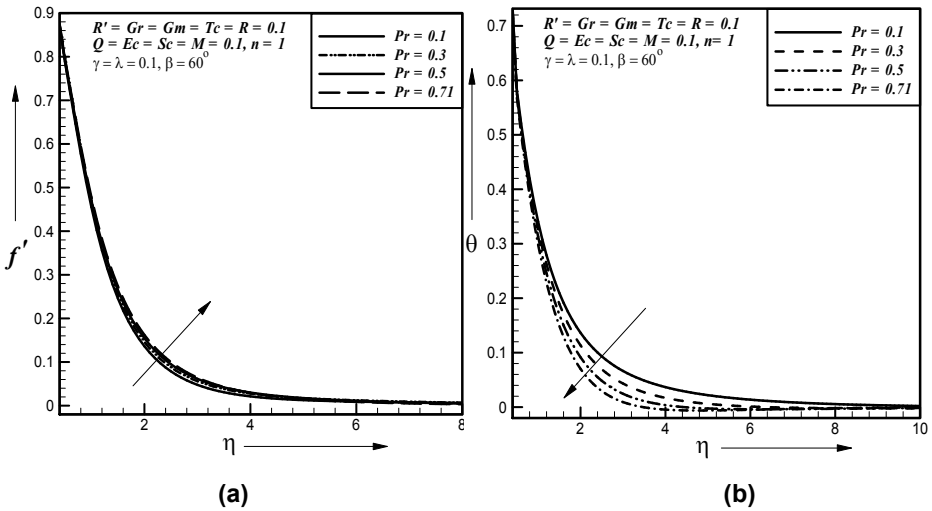

Fig. 8. Effect of Prandtl number on a) primary velocity b) temperature profiles

In Figs. 11a-11b and 12a-12b, primary shear stress decreases but secondary shear stress increases with the increase of magnetic parameter and heat source parameter (Q) respectively.

Figs. 13a and 13b represent that primary shear stress decreases but secondary shear stress increases with the increase ofporosity parameter.

In Fig. 14a and Fig. 14b, primary shear stress increases with the increase ofGrashof number and modified Grashof number respectively.

In Fig. 15a, primary shear stress decreases with the increase ofinclination angle. In Fig. 15b, the heat transfer rate increases with the increase ofthermal conductivity parameter. Fig. 16a, the heat transfer rate decreases with the increase ofPrandtl number. Fig. 16b, the heat transfer rate increases with the increase ofheat source parameter.

In Fig. 17a -17b, the heat transfer rate increases with the increase ofEckert number andradiation parameter. Fig. 18a -Fig. 18b, the mass transfer rate decreases with the increase ofSchmidt number and reaction parameter. Fig. 19 represents that the mass transfer rate increases with the increase oforder of chemical reaction parameter.

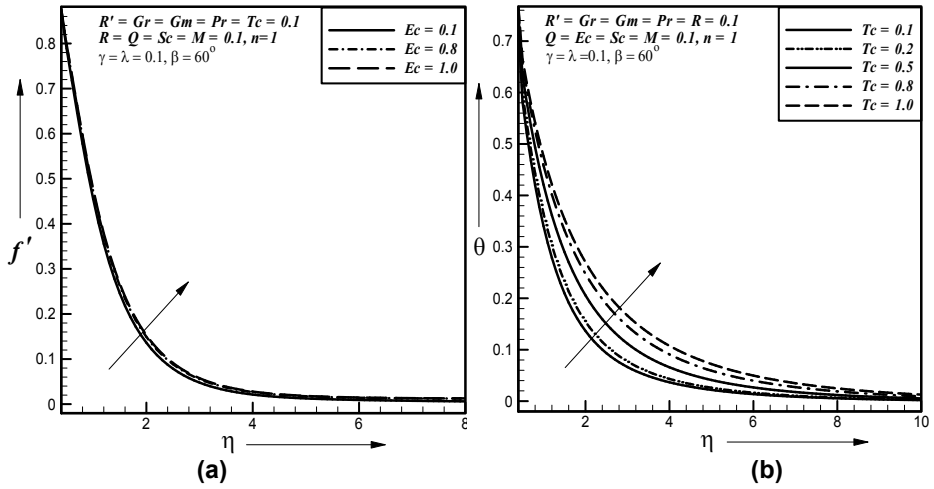

Fig. 9. Effect of a) Eckert number on primary velocity profiles b) thermal conductivity parameter on temperature profiles

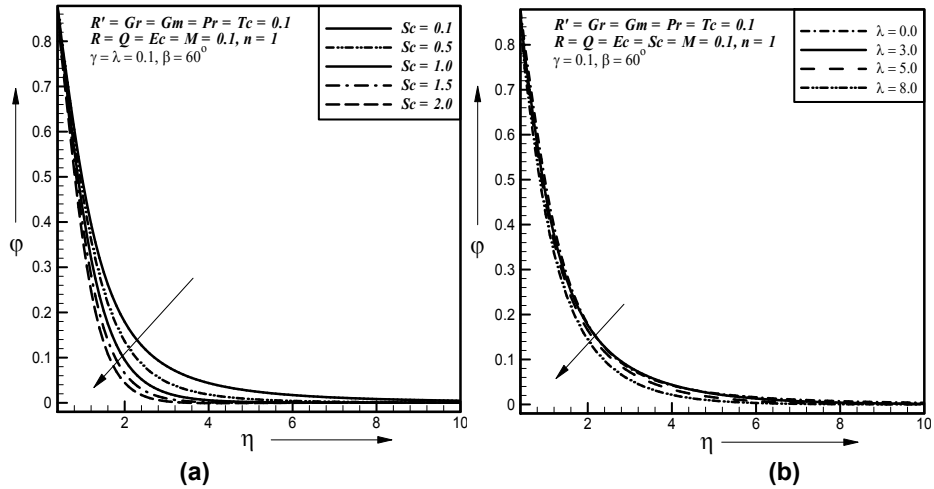

Fig. 10. Effect of a) Schmidt number on concentration profiles b) reaction parameter on concentration profiles

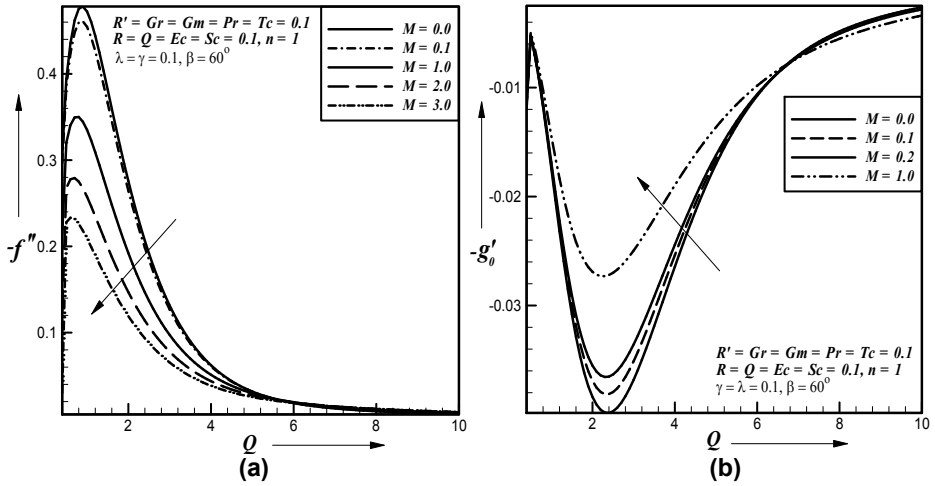

Fig. 11. Effect of magnetic parameter on a) primary shear stress b) secondary shear stress

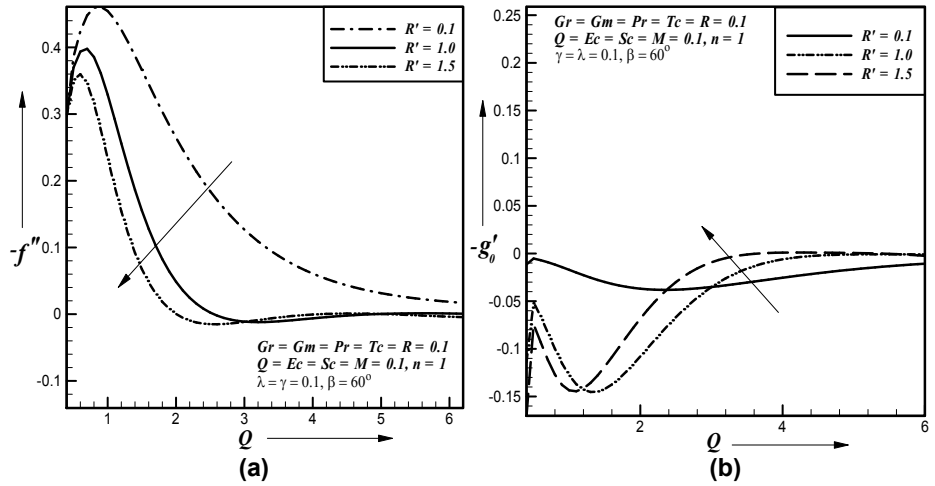

Fig. 12. Effect of rotational parameter on a) primary shear stress b) secondary shear stress

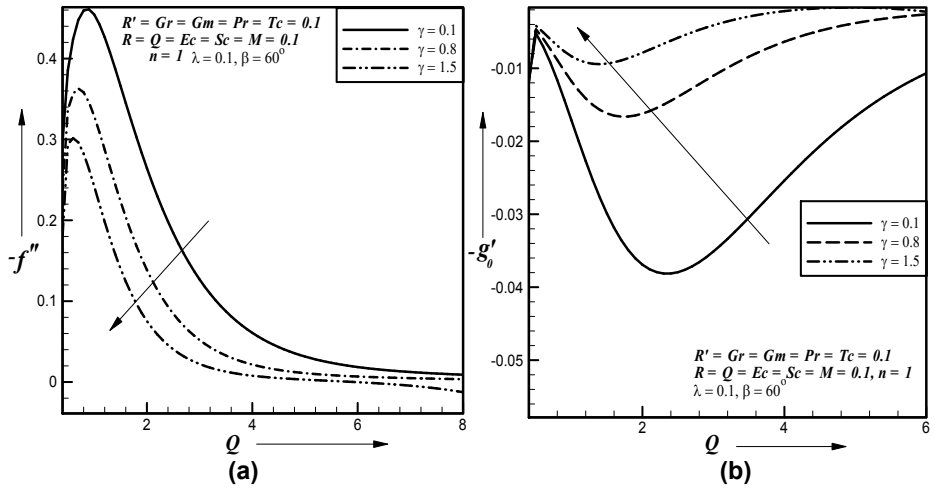

Fig. 13. Effect of porosity parameter on a) primary b) secondary shear stress

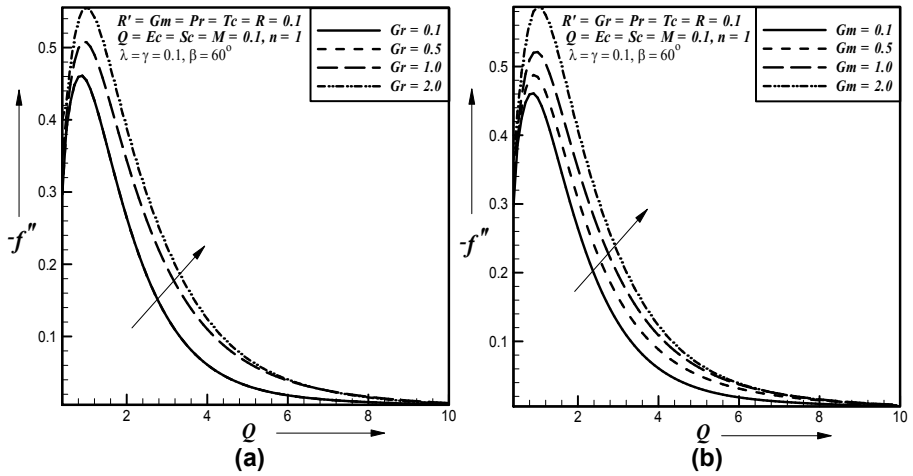

Fig. 14. Effect of a) grashof number b) modified grashof on primary shear stress

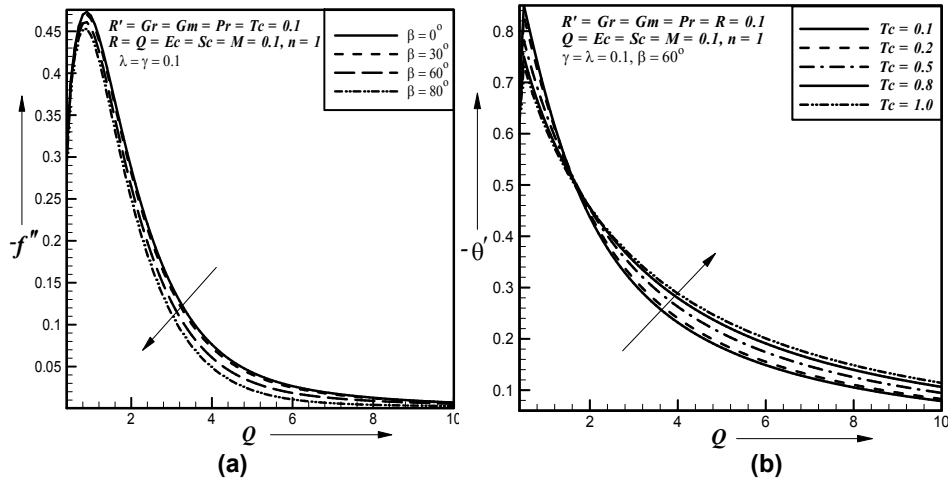

Fig. 15. Effect of a) inclination angle on primary shear stress b) thermal conductivity parameter on heat transfer rate

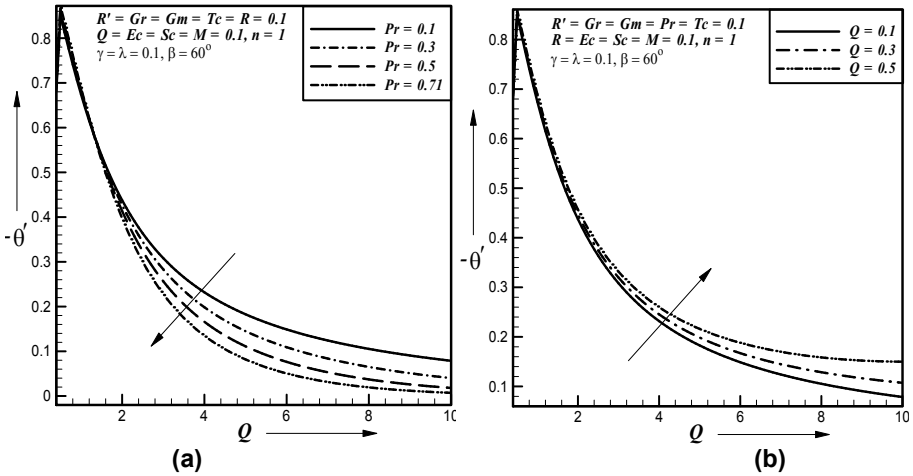

Fig. 16. Effect of a) prandtl number b) heat source parameter on heat transfer rate

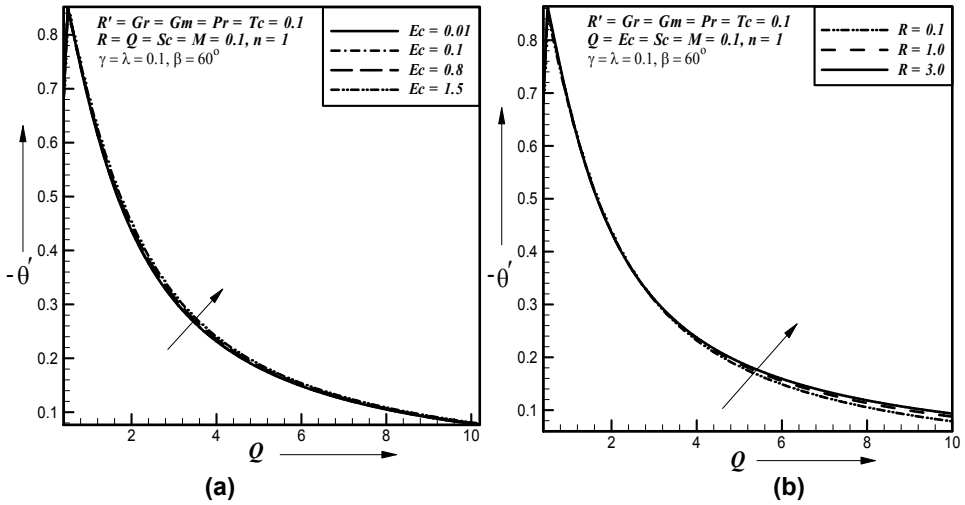

Fig. 17. Effect of a) Eckert number b) radiation parameter on heat transfer rate

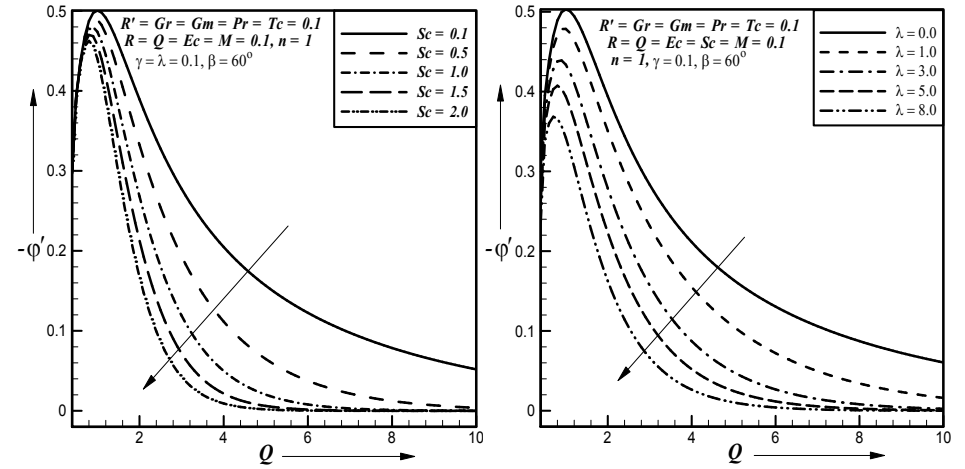

Fig. 18. Effect of a) Schmidt number b) reaction parameter on mass transfer rate

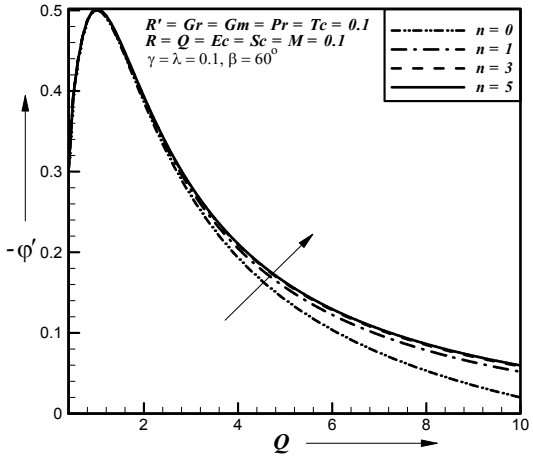

Fig. 19. Effect of order of chemical reaction on mass transfer rate

4. CONCLUSION

Primary velocity profiles decreases and primary shear stress with the increase of magnetic parameter, rotational parameter, but reverse effect is found for the secondary velocity profiles and secondary shear stress. Primary shear stress decreases due to increase of magnetic parameter where as the reverse effect is found for secondary shear stress.

Temperature and concentration boundary layer thickness increases due to increase of rotational parameter.

The primary velocity profiles and primary shear stress decreases due to increase of permeability of the porous medium and inclination angle but reverse effect is found for the secondary velocity profiles and secondary shear stress. Temperature and concentration boundary layer thickness are increases due to increase of permeability of the porous medium.

The primary velocity profiles and primary shear stress increases due to increase of Grashof number where as the reverse effect is found for the secondary velocity profiles. Also the temperature boundary layer thickness is decreases due to increase of Grashof number.

The primary velocity profiles and primary shear stress increases due to increase of modified Grashof number where as the reverse effect is found for the secondary velocity profiles. Also the concentration boundary layer thickness decreases due to increase of modified Grashof number.

The primary velocity profiles increases due to increase of Prandtl number. The thermal boundary layer thickness as well as the heat transfer rate at the plate decreases as the Prandtl number increases.

The heat transfer rate at the plate as well as the primary velocity is increases due to increase of Eckert number and thermal conductivity parameter.

The heat transfer rate at the plate increases due to increase of heat source parameter and radiation parameter.

The concentration boundary layer thickness as well as the mass transfer rate at the plate decreases due to increase of Schmidt number, no reaction and destructive reaction.

The mass transfer rate at the plate increases due to increase of order of chemical reaction.

COMPETING INTERESTS

Authors have declared that no competing interests exist.

REFERENCES

1. Bluman GW, Kumei S. Symmetries and Differential Equations. Springer-verlag: New York; 1989.
2. Helmy KA. MHD boundary layer equations for power law fluids with variable electric conductivity. Mechanica. 1995;30:187-200.
3. Pakdemirli M, Yurusoy M. Similarity transformations for partial differential equations. SIAM Review. 1998;40:96-101.
4. Kalpakides VK, Balassas KB. Symmetry groups and similarity solutions for a free convective boundary-layer problem. International Journal of Non-Linear Mechanics. 2004;39:1659-1670.
5. Makinde OD. Free convection flow with thermal radiation and mass transfer past moving vertical porous plate. International Communications in Heat and Mass Transfer. 2005;32:1411-1419.
6. Seddeek MA, Salem AM. Laminar mixed convection adjacent to vertical continuously stretching sheet with variable viscosity and variable thermal diffusivity. Heat and Mass Transfer. 2005;41:1048-1055.
7. Ibrahim FS, Elaiw AM, Bakr AA. Effect of the chemical reaction and radiation absorption on the unsteady MHD free convection flow past a semi infinite vertical permeable moving plate with heat source and suction. Communications in Nonlinear Science and Numerical Simulation. 2008;13:1056-1066.
8. El-Kabeir SMM, El-Hakiem MA, Rashad. Lie group analysis of unsteady MHD three dimensional dimensional by natural convection from an inclined stretching surface saturated porous medium. Journal of Computational and Applied Mathematics. 2008;213:582-603.
9. Rajeswari R, Jothiram J, Nelson VK. Chemical Reaction, Heat and Mass Transfer on Nonlinear MHD Boundary Layer Flow through a Vertical Porous

Surface in the Presence of Suction. Applied Mathematical Sciences. 2009;3:2469-2480.

10. Chandrakala P. Chemical reaction effects on MHD flow past an impussively started semi-infinite vertical plate. International Journal of Dynamics of Fluids. 2010;6:77-79.
11. Joneidi AA, Domairry G, Balaelahi M. Analytical treatment of MHD free convective flow and mass transfer over a stretching sheet with chemical reaction. Journal of the Taiwan Institute of Chemical Engineers. 2010;41:35-43.
12. Muhaimin, Kandasamy R, Hashim I. Effect of chemical reaction, heat and mass transfer on nonlinear boundary layer past a porous shrinking sheet in the presence of suction. Nuclear Engineering and Design. 2010;240(5):933-939.
13. Rahman MM, Salahuddin KM. Study of hydromagnetic heat and mass transfer flow over an inclined heated surface with variable viscosity and electric conductivity. Communications in Nonlinear Science and Numerical Simulation. 2010;15:2073-2085.
14. FerdowsM, Khan MS, Alam MM, Sun S. MHD Mixed convective boundary layer flow of a nanofluid through a porous medium due to an Exponentially Stretching sheet. Mathematicalproblems in Engineering. 2012;3(7):1-21.
15. Khan MS, Wahiduzzaman M, Sazad MAK, Uddin MS. Finite difference solution of MHD free convection heat and mass transfer flow of a nanofluid along a Stretching sheet with Heat generation effects. Indian Journal of Theoretical Physics. 2012;60(4):285-306.
16. Khan MS, Karim I, Biswas MHA. Non-Newtonian MHD Mixed Convective Power-Law Fluid Flow over a Vertical Stretching Sheet with Thermal Radiation, Heat Generation and Chemical Reaction Effects. Academic Research International. 2012;3(3):80-92.
17. Khan MS, Karim I, Ali LE, Islam A. MHD Free Convection Boundary layer Unsteady Flow of a Nanofluid along a stretching sheet with thermal Radiation and Viscous Dissipation Effects. International Nano Letters. 2012;24(2):1-9.
18. Khan MS, Karim I, Biswas MHA. Heat Generation, Thermal Radiation and Chemical Reaction Effects on MHD Mixed Convection Flow over an Unsteady Stretching Permeable Surface. International Journal of Basic and Applied Science. 2012;1(2):363-377.
19. Beg OA, Khan MS, Karim I, Alam MM, Ferdows M. Explicit Numerical study of Unsteady Hydromagnetic Mixed Convective Nanofluid flow from an Exponential Stretching sheet in Porous media. Applied Nanoscience. 2013;4(8):943-957.
20. Khan MS, Alam MM, Ferdows M. Effects of Magnetic field on Radiative flow of a Nanofluid past a Stretching Sheet. Procedia Engineering. 2013;56:316-322.
21. Ferdows M, Khan MS, Bég OA, Alam MM. Numerical Study of Transient Magnetohydrodynamic Radiative Free Convection Nanofluid Flow from A Stretching Permeable Surface. Journal of Process Mechanical Engineering. 2014;Sep25:1-16.
22. Khan MS, Karim I, Islam MS. Possessions of Chemical Reaction on MHD Heat and Mass Transfer Nanofluid Flow on a Continuously Moving Surface. American Chemical Science Journal. 2014;4(3):401-415.
23. Karim I, Islam MS, Khan MS. MHD Buoyancy Flows of Cu, Al_2O_3 and TiO_2 nanofluid near Stagnation-point on a Vertical Plate with Heat Generation. Physical Science International Journal. 2014;4(6):754-767.
24. Khan MS, Wahiduzzaman M, Karim I, Islam MS, Alam MM. Heat Generation Effects on Unsteady Mixed Convection Flow from a Vertical Porous Plate with Induced Magnetic Field. Procedia Engineering. 2014;90:238-244.
25. Khan MS, Karim I, Islam MS, Wahiduzzaman M. MHD Boundary Layer Radiative, Heat Generating and Chemical Reacting Flow past a Wedge Moving in a Nanofluid. Nano Convergence. 2014;20(1):1-13.
26. Wahiduzzaman M, Khan MS, Karim I. MHD convective stagnation flow of nanofluid over a shrinking surface with thermal radiation, heat generation and chemical reaction. Accepted, Procedia Engineering; 2015.

27. Wahiduzzaman M, Khan MS, Karim I, Biswas P, Uddin MS. Viscous Dissipation and Radiation effects on MHD Boundary Layer Flow of a Nanofluid past a Rotating Stretching Sheet. Accepted, Applied Mathematics; 2015.

Peer-review history:
The peer review history for this paper can be accessed here:
http://www.sciencedomain.org/review-history.php?iid=1000&id=33&aid=8271